

Local Differential Privacy for Molecular Communication Networks

Melih Şahin , *Graduate Student Member, IEEE*, Ozgur B. Akan , *Fellow, IEEE*

Abstract—Molecular communication (MC) enables information exchange in nanoscale sensor networks operating in biological environments, yet privacy remains largely unaddressed. We integrate local differential privacy (LDP) into diffusion-based MC by privatizing each user’s measurement at the transmitter and conveying the resulting randomized report over the MC channel. To our knowledge, this is the first systematic LDP implementation for diffusion-based MC, enabling privacy-preserving aggregate data analysis for in-body health monitoring and other population-scale sensing applications. We benchmark major LDP mechanisms under a realistic channel model. Simulation results show that k-ary Randomized Response (KRR) and Optimized Local Hashing (OLH) achieve the lowest average ℓ_1 distribution-estimation error under the MC channel: OLH is preferable when channel resources are sufficient and the number of possible user values (alphabet size) k is moderate to large, whereas the KRR is more robust as the MC transmission quality deteriorates. We further propose RLIM-LDP, which combines run-length-limited ISI-mitigation (RLIM) coding with LDP coding. Extensive simulation results demonstrate that RLIM-LDP improves end-to-end reliability and reduces the final distribution-estimation error when time and molecule resources are limited.

Index Terms—Biological networks, molecular communication, local differential privacy, channel coding, diffusion channels

I. INTRODUCTION

Diffusion-based molecular communication (MC) uses the controlled release, propagation, and detection of molecules to convey information in fluidic media where electromagnetic communication can be unreliable or impractical [1]. This makes MC a natural candidate for communication among nanoscale devices in diffusive biological environments, such as the human vascular system.

Privately transmitting individual information at population scale is an important task, especially when the data contains highly personal information. In MC, security and privacy have been highlighted as major open challenges, with early work outlining MC-specific attack methods and noting that conventional cryptographic defenses may be impractical at the nano/micro-scale [2]. Recent efforts also explore information-theoretic secure communication viewpoints for Poisson models

motivated by medical MC [3]. However, beyond defending against external adversaries, many in-body health-monitoring scenarios require a stronger notion of privacy in which even the data collector should not be able to reliably infer any individual’s sensitive value.

A rigorously-defined way to privately send information, in the sense that privacy is protected even from the receiver itself, is through local differential privacy (LDP) [4]. The output of each user is randomized based on the LDP mechanism used. This gives the user plausible deniability and thus ensures privacy. Once sufficiently many users send privatized reports, the receiver can estimate the underlying distribution. A central purpose of LDP is therefore to enable aggregate data analysis while preserving individual privacy. In this work, we focus on the fundamental LDP problem of estimating a k -ary probability distribution when N users report privatized messages to a central server. For instance, each of these N subjects may be a human, and the report may be an important biological trait: in the simplest case, the presence or absence of a disease, where the aim is to estimate the prevalence of that disease among the general public, without endangering personal privacy.

Performance comparisons of major LDP schemes are well documented in the literature [4], [5]. However, in the resource-constrained setting of MC, the communication cost (both the length of the transmitted binary string and the number of 1-bits it contains) can significantly affect communication quality [6]. Since MC has strong potential for enabling in-vivo body communication, it is therefore important to compare existing LDP schemes specifically in the context of an MC channel. To the best of our knowledge, this is the first work to provide such a comparison.

The remainder of this paper is organized as follows. Section II introduces the system model for the diffusion-based molecular communication channel. Section III details the local differential privacy architecture and outlines the state-of-the-art LDP mechanisms evaluated in this study. In Section IV, we present our simulation framework and provide a comparative performance analysis of these privacy schemes under realistic MC channel conditions. To further enhance communication reliability and minimize distribution-estimation error, Section V proposes the RLIM-LDP framework, which combines run-length-limited ISI-mitigation coding [6] with LDP coding. Finally, Section VI concludes the paper.

II. MOLECULAR COMMUNICATION CHANNEL

The classical SISO (single-input single-output) molecular communication system is shown in Fig. 1. The information

Melih Şahin is with the Internet of Everything (IoE) Group, Department of Engineering, University of Cambridge, CB3 0FA Cambridge, U.K. (e-mail: ms3195@cam.ac.uk).

Ozgur B. Akan is with the Internet of Everything (IoE) Group, Department of Engineering, University of Cambridge, CB3 0FA Cambridge, U.K., and also with the Center for neXt-generation Communications (CXC), Department of Electrical and Electronics Engineering, Koç University, 34450 Istanbul, Türkiye (e-mail: oba21@cam.ac.uk).

M. Şahin’s work was supported in part by the TÜBİTAK BİDEB 2213-A Scholarships programme.

This work was supported in part by the AXA Research Fund (AXA Chair for Internet of Everything at Koç University).

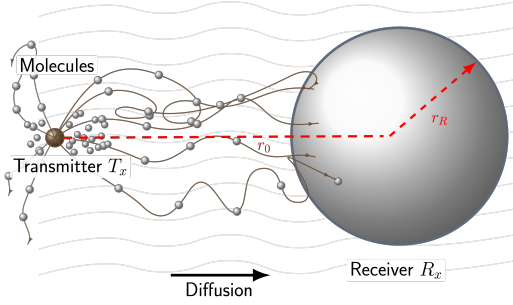


Fig. 1: MC Channel Model

is transmitted using binary concentration shift keying (BCSK) modulation [7] with a fully absorbing spherical receiver: The time axis is divided into equally long signal intervals (i.e., time slots). In each signal interval, a single bit (either a 0-bit or a 1-bit) is transmitted. If a 1-bit is to be transmitted, at the start of the corresponding signal interval, M molecules are released from the transmitter and diffuse via Brownian motion [8]. If a 0-bit is to be transmitted, no molecules are emitted from the transmitter. Some of these M molecules may be detected (i.e., absorbed) by the receiver within the current interval, within ensuing intervals, or not be detected at all. The receiver counts the number of molecules it absorbs within each signal interval. Therefore, in a SISO MC model, for a binary sequence of length n , we obtain a nonnegative integer sequence of length n .

The probability of a single molecule released from the transmitter getting absorbed by the receiver within time t (in s) is given by [9]:

$$F(t) = \frac{r_R}{r_0} \operatorname{erfc}\left(\frac{r_0 - r_R}{\sqrt{4Dt}}\right), \quad (1)$$

where D is the diffusion coefficient (in $\mu\text{m}^2/\text{s}$), r_R is the receiver radius (in μm), and r_0 denotes the transmitter–receiver distance (center-to-center) in μm .

As emphasized before, for $i \in \mathbb{N}$, a molecule released at the start of a given signal interval may get absorbed within that interval or within any of the ensuing signal intervals. The i -th channel coefficient is defined as the probability that a single molecule released at the start of the j -th signal interval gets absorbed within the $(j + i - 1)$ -th signal interval, and it is given by

$$p_i = F(i \cdot t_s) - F((i - 1) \cdot t_s), \quad (2)$$

for signal interval duration t_s (in s) [1].

For a transmitted 1-bit, each of the M emitted molecules falls into exactly one of the following mutually exclusive outcomes: it is absorbed in the 1st, 2nd, \dots , I -th subsequent signal interval, or it is not absorbed within the modeled memory window (i.e., it arrives later than I intervals, or it never arrives). Thus, for a single emission event, the vector of molecule counts across these outcomes follows a multinomial distribution [10]:

$$(X_1, \dots, X_I, X_{I+1}) \sim \text{Multinomial}(M; p_1, \dots, p_I, p_{I+1}), \quad (3)$$

where X_i denotes the number of molecules absorbed in the i -th interval after emission (relative to the emission time), and

$$p_{I+1} = 1 - \sum_{i=1}^I p_i \quad (4)$$

collects the probability mass of molecules that are not absorbed within the first I intervals. The constant I is introduced to simulate the MC channel under constrained computational resources by truncating the channel memory. When I is chosen sufficiently large, this truncation causes only a slight deviation from the most accurate (i.e., $I = n$) model, since the coefficients p_i rapidly decay as i increases, and the remaining tail probability becomes negligible. Then, for a transmitted binary sequence $\{b_j\}_{j=1}^n$ with $b_j \in \{0, 1\}$, the received molecule count in the h -th interval can be modeled as

$$N_h = \sum_{i=1}^{\min\{h, I\}} b_{h-i+1} X_i^{(h-i+1)} + W, \quad (5)$$

where $X_i^{(m)}$ is the multinomial component [10] corresponding to molecules emitted in interval m and absorbed i intervals later, and W denotes receiver counting noise. In our simulations, additive Gaussian noise with variance σ^2 and mean 0, rounded to the nearest integer, has been used.

III. LDP SYSTEM MODEL

In a typical local differential privacy (LDP) model [4], it is assumed that there are N entities sending information to a central server for aggregate data analysis. While in the classical definition of differential privacy this central server is assumed to be trusted and secure, LDP assumes that even the central server may not be secure (i.e., it may be curious or untrusted). Aggregate data processing is used for many different purposes, such as machine learning data collection, large-scale data analytics, public health monitoring, and privacy-preserving surveys or censuses, where only population-level frequencies are needed.

A central benchmark for evaluating an LDP mechanism is the problem of k -ary probability distribution estimation [4]. In the k -ary distribution estimation problem, each user holds a categorical value $X \in [k] = \{1, 2, \dots, k\}$ drawn i.i.d. from an unknown distribution

$$\mathbf{p} \in S_k = \left\{ \mathbf{p} \in \mathbb{R}^k : p_i \geq 0, \sum_{i=1}^k p_i = 1 \right\}, \quad (6)$$

where S_k denotes the probability simplex. An LDP mechanism is defined by an output alphabet Y and a conditional distribution (equivalently, a probabilistic matrix)

$$Q \in [0, 1]^{k \times |Y|}, \quad Q_{x,y} = \Pr(Y = y | X = x), \quad (7)$$

where Y is the output space of the mechanism. That is, for each input $x \in [k]$, the mechanism outputs a randomized report $y \in Y$ according to the distribution given by the x -th row of Q .

An LDP mechanism is ϵ -locally differentially private iff for all $x, x' \in [k]$ and for all $y \in Y$,

$$\frac{\Pr(Y = y | X = x)}{\Pr(Y = y | X = x')} \leq e^\epsilon, \quad (8)$$

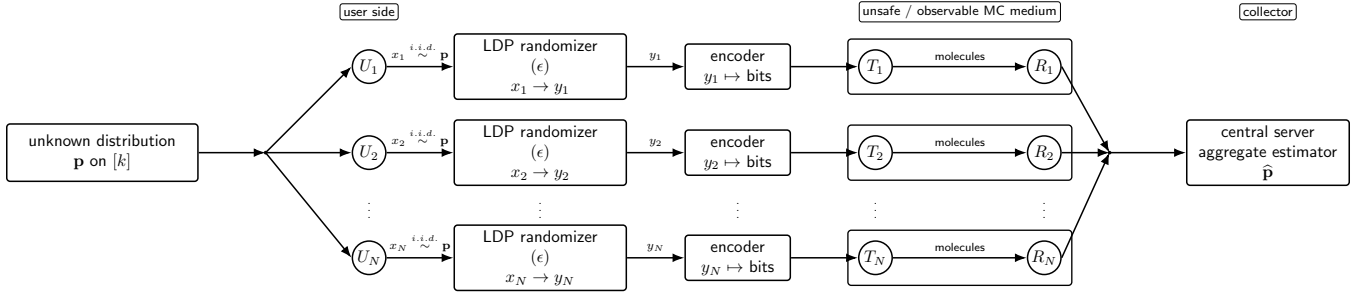


Fig. 2: Network architecture for local differential privacy in molecular communication

where ϵ is a nonnegative real number [4]. Smaller values of ϵ provide a higher degree of privacy. For instance, $\epsilon = 0$ corresponds to perfect privacy. However, in that case, the privatized reports carry essentially no useful information, so meaningful estimation of \mathbf{p} is not possible.

We demonstrate our privacy model for MC in Fig. 2. In this architecture, there are N subjects (e.g., human users), each equipped with an in-body sensor–gateway pair. For subject $i \in [N]$, the in-body sensor node T_i (equipped with sensing and molecular transmission capability) observes a value $x \in [k]$, privatizes it by randomly choosing $y \in Y$ according to $\Pr(Y = y | X = x)$, and transmits a binary representation of y over a diffusion-based MC link. The receiver R_i detects (absorbs/counts) the molecular signal and then forwards the decoded report to a distant central server using classical electromagnetic (EM) communication with negligible error.

While electromagnetic (EM) links are feasible for many implants, direct EM transmission from T_i may be unreliable or undesirable in the specific regime we consider due to strong tissue-dependent attenuation, antenna size constraints at the nano/micro-scale (wavelength-scale effects), and strict power/thermal budgets [11]. In such short-range, fluidic biological environments (e.g., intravascular or interstitial media), chemically mediated diffusion can be a more compatible in-body physical layer; our focus is therefore the regime where an MC channel $T_i \rightarrow R_i$ is necessary.

It may be argued that privatization could instead be performed at the gateway side R_i . However, we do not assume the MC channel is trusted: besides the intended receiver, adversarial nano/micro-scale entities in the environment may observe the molecular signal. In addition to this, the gateway R_i itself may be untrusted in some deployments. Therefore, to provide an end-to-end local privacy guarantee independent of the receiver, privatization is performed at the sensor-transmitter side T_i . We now present the standard LDP schemes used in the literature as follows:

A. The k -ary Randomized Response (KRR)

In KRR [12], the output alphabet is the same as the input, i.e., $Y = [k]$. Given a symbol $x \in [k]$, the user reports

$$Y = \begin{cases} x, & \text{with prob. } p, \\ y \neq x \text{ uniformly over } [k] \setminus \{x\}, & \text{with prob. } 1 - p, \end{cases} \quad (9)$$

where $p = \frac{e^\epsilon}{e^\epsilon + k - 1}$. The server receives N reports Y_1, \dots, Y_N and forms the empirical histogram $\hat{f}_j = \frac{1}{N} \sum_{i=1}^N \mathbf{1}\{Y_i = j\}$. An unbiased estimate (i.e., $\mathbb{E}[\hat{p}_j] = p_j$ for all $j \in [k]$) of the underlying distribution is then given as:

$$\hat{p}_j = \frac{\hat{f}_j - q}{p - q}, \quad q = \frac{1}{e^\epsilon + k - 1}. \quad (10)$$

B. Basic RAPPOR (Symmetric Unary Encoding)

Basic RAPPOR [13] represents the input $x \in [k]$ as a unary (i.e., containing only one 1-bit) vector $\mathbf{v} \in \{0, 1\}^k$ with $v_x = 1$ and $v_j = 0$ for $j \neq x$. The user then flips each bit independently: a 1 stays 1 with probability p (and flips to 0 with probability $1 - p$), while a 0 flips to 1 with probability q . In basic RAPPOR,

$$p = \frac{e^{\epsilon/2}}{e^{\epsilon/2} + 1}, \quad q = \frac{1}{e^{\epsilon/2} + 1}. \quad (11)$$

Let $\mathbf{z}_i \in \{0, 1\}^k$ be the privatized vector from user i , and define the average $\bar{z}_j = \frac{1}{N} \sum_{i=1}^N z_{i,j}$. The unbiased estimator is as follows:

$$\hat{p}_j = \frac{\bar{z}_j - q}{p - q}. \quad (12)$$

C. Optimized Unary Encoding (OUE)

OUE [4] uses the same unary representation as basic RAPPOR, but chooses parameters to reduce estimation variance. Again the user encodes x as a one-hot vector $\mathbf{v} \in \{0, 1\}^k$, and flips bits independently with probabilities p (for the true 1-bit) and q (for 0-bits). In OUE,

$$p = \frac{1}{2}, \quad q = \frac{1}{e^\epsilon + 1}. \quad (13)$$

The unbiased estimator is the same form as in basic RAPPOR:

$$\hat{p}_j = \frac{\bar{z}_j - q}{p - q}, \quad \bar{z}_j = \frac{1}{N} \sum_{i=1}^N z_{i,j}. \quad (14)$$

D. Binary Local Hashing (BLH)

In BLH [4], each $x \in [k]$ is identified with its binary representation $\mathbf{x} \in \{0, 1\}^d$, where $d = \lceil \log_2 k \rceil$. The user draws a random hash vector $\mathbf{r} \in \{0, 1\}^d$ uniformly and computes the hashed bit

$$t = \langle \mathbf{r}, \mathbf{x} \rangle \bmod 2 = \left(\sum_{i=1}^d r_i \cdot x_i \right) \bmod 2. \quad (15)$$

Then the user applies binary randomized response to t : the reported bit equals t with probability $p = \frac{e^\epsilon}{e^\epsilon + 1}$, and is flipped otherwise. The transmitted report is the pair (\mathbf{r}, Y) , where $Y \in \{0, 1\}$ is the randomized reported bit.

At the server, for each candidate $v \in [k]$ with binary form \mathbf{v} , we check whether each received report matches the predicted hash, i.e., whether $Y_i = \langle \mathbf{r}_i, \mathbf{v} \rangle \bmod 2$. Let

$$c_v = \frac{1}{N} \sum_{i=1}^N \mathbf{1}\{Y_i = \langle \mathbf{r}_i, \mathbf{v} \rangle \bmod 2\}. \quad (16)$$

Note that $\mathbb{E}[c_v] = p_v p + (1 - p_v) \cdot \frac{1}{2}$, where $p_v = \Pr(X = v)$. The $\frac{1}{2}$ comes from the fact that for $X \neq v$ we have $\mathbf{x} \oplus \mathbf{v} \neq \mathbf{0}$, so with uniform \mathbf{r} the bit $\langle \mathbf{r}, \mathbf{x} \rangle \bmod 2$ matches $\langle \mathbf{r}, \mathbf{v} \rangle \bmod 2$ with probability $\frac{1}{2}$, and randomized response cannot change this symmetry. Thus an unbiased estimator is as follows:

$$\hat{p}_v = \frac{c_v - 1/2}{p - 1/2}.$$

E. Optimized Local Hashing (OLH)

OLH [4] is the g -ary analogue of BLH: instead of hashing to one bit, we hash to an alphabet of size g and then apply g -ary randomized response. The transmitted report is (h, Y) , where $h : [k] \rightarrow [g]$ is a randomly chosen hash function and $Y \in [g]$ is the randomized hash output.

The crucial requirement is the following symmetry: for a given family of hash functions H and for any two distinct symbols $x \neq v$,

$$\Pr_{h \in H}(h(x) = h(v)) = \frac{1}{g}. \quad (17)$$

This is the exact g -ary counterpart of the $\frac{1}{2}$ symmetry in BLH. The choice of g directly determines the estimation variance. This variance is given below:

$$V(g; \epsilon) \propto \frac{(e^\epsilon - 1 + g)^2}{(e^\epsilon - 1)^2 (g - 1)}, \quad g \geq 2. \quad (18)$$

This is minimized at the continuous optimum $g = e^\epsilon + 1$. Universal hash families H satisfying (17) are known to exist whenever g is a prime power, because a finite field with g elements (denoted $\text{GF}(g)$) exists in that case. Such constructions typically use arithmetic over $\text{GF}(g)$ (e.g., polynomial-based maps), which is more involved to implement on a severely constrained nano/micro-scale transmitter. In our MC setting, we therefore use a modulo-based construction that achieves (17) using only integer arithmetic, which requires g to be *prime* (so that \mathbb{Z}_g is a field). Thus, in our paper, we choose g in the following way: Let $g_0 = \lceil e^\epsilon \rceil + 1$, take the nearest primes below and above g_0 : $g^- = \max\{q \leq g_0 : q \text{ prime}\}$ and $g^+ = \min\{q \geq g_0 : q \text{ prime}\}$; and set

$$g = \arg \min_{q \in \{g^-, g^+\}} V(q; \epsilon).$$

Then, let $m = \lceil \log_g k \rceil$ and represent each $x \in [k]$ by its length- m base- g vector $\mathbf{x} \in \{0, 1, \dots, g-1\}^m$. The user samples $\mathbf{r} \in \{0, 1, \dots, g-1\}^m$ uniformly and defines the hash

$$h_{\mathbf{r}}(x) = \langle \mathbf{r}, \mathbf{x} \rangle \bmod g = \left(\sum_{j=1}^m r_j x_j \right) \bmod g. \quad (19)$$

Whenever g is prime and \mathbf{r} is uniformly chosen, this family satisfies (17), since for any $x \neq v$ the random variable $\langle \mathbf{r}, \mathbf{x} - \mathbf{v} \rangle \bmod g$ is uniform over $[g]$.

Given $t = h(x) \in [g]$, the user applies g -ary randomized response:

$$\Pr(Y = t) = p, \quad p = \frac{e^\epsilon}{e^\epsilon + g - 1}. \quad (20)$$

Otherwise, it outputs a symbol chosen uniformly from $[g] \setminus \{t\}$, i.e.,

$$\Pr(Y = y) = \frac{1 - p}{g - 1}, \quad \forall y \in [g] \setminus \{t\}. \quad (21)$$

This provides us with ϵ -local privacy. The report (h, Y) is then transmitted. Since our diffusion-based MC model uses binary modulation, before transmitting $(h, Y) \in [g]^{m+1}$, we map it to an integer $z \in \{0, \dots, g^{m+1} - 1\}$ via its base- g expansion (with $(0, \dots, 0) \mapsto 0$ and counting upward), and transmit the fixed-length binary representation of z with $\lceil \log_2(g^{m+1}) \rceil$ bits.

At the server, for each candidate $v \in [k]$, define

$$c_v = \frac{1}{N} \sum_{i=1}^N \mathbf{1}\{Y_i = h_i(v)\}. \quad (22)$$

Using (17), one obtains $\mathbb{E}[c_v] = p_v \cdot p + (1 - p_v) \cdot \frac{1}{g}$. Hence, for each $v \in [k]$, an unbiased estimator is

$$\hat{p}_v = \frac{c_v - 1/g}{p - 1/g}. \quad (23)$$

F. Hadamard Response (HR)

Hadamard Response (HR) [14] achieves strong accuracy guarantees while enabling fast server-side frequency estimation. For brevity, we detail the core HR mechanism optimized for the high-privacy regime ($\epsilon = O(1)$) below. In our simulations for $\epsilon > 1$, we implement the generalized block-structured HR construction detailed in Appendix A of [14], which maintains sample optimality by dynamically scaling the subset size.

Let k be the domain size and set $K = \lceil \log_2(k+1) \rceil$, $d = 2^K$. Identify each $j \in [d]$ with its K -bit binary vector (and similarly for $t \in [d]$). Define the Hadamard matrix $H \in \{\pm 1\}^{d \times d}$ by

$$H_{j,t} = (-1)^{\langle j, t \rangle}, \quad (24)$$

where $\langle j, t \rangle$ is the (mod-2) inner product of the two K -bit vectors.

Given input $x \in [k]$, define the associated ‘‘positive-support’’ index set

$$S_x = \{j \in [d] : H_{x+1,j} = +1\}, \quad (25)$$

(where the column index $x+1$ is used so that $x \in [k]$ maps into $\{1, \dots, k\} \subset [d]$). Note that $|S_x| = d/2$ for every x ; and, for all $x \neq y \in [k]$, $|S_x \cap S_y| = |S_x - S_y| = d/4$.

The HR local randomizer outputs $Y \in [d]$ as follows. Let

$$p = \frac{e^\epsilon}{e^\epsilon + 1}. \quad (26)$$

With probability p , sample Y uniformly from S_x ; with probability $1 - p$, sample Y uniformly from $[d] \setminus S_x$. Equivalently,

$$\Pr(Y = j \mid X = x) = \begin{cases} \frac{p}{|S_x|} = \frac{2p}{d}, & j \in S_x, \\ \frac{1-p}{d-|S_x|} = \frac{2(1-p)}{d}, & j \notin S_x. \end{cases} \quad (27)$$

This satisfies ϵ -LDP since the maximum likelihood ratio is $\frac{p}{1-p} = e^\epsilon$.

At the server, for each candidate $v \in [k]$, define

$$c_v = \frac{1}{N} \sum_{i=1}^N \mathbf{1}\{Y_i \in S_v\}. \quad (28)$$

Then $\Pr(Y \in S_v \mid X = v) = p$ and for all $x \neq v$ $\Pr(Y \in S_v \mid X = x) = \frac{d-2p}{4} + \frac{d-2(1-p)}{4} = \frac{1}{2}$, hence $\mathbb{E}[c_v] = p_v p + (1 - p_v) \frac{1}{2}$. Therefore an unbiased estimator is

$$\hat{p}_v = \frac{c_v - \frac{1}{2}}{p - \frac{1}{2}} = \frac{2(e^\epsilon + 1)}{e^\epsilon - 1} \left(c_v - \frac{1}{2} \right). \quad (29)$$

A primary benefit of HR is its low server-side time complexity, which is achieved through the fast multiplication property of Hadamard matrices. However, this advantage is not strictly necessary in our system model. We assume the central data collector is computationally unconstrained, shifting the focus entirely to the resource limitations of the molecular transmitters.

IV. SIMULATION

A. Simulation Mechanism

We now compare the LDP mechanisms of Section III under the diffusion-based MC channel of Section II across a broad range of scenarios. Unless stated otherwise, we use $D = 79.4 \mu\text{m}^2/\text{s}$, $r_R = 5 \mu\text{m}$, $r_0 = 10 \mu\text{m}$ ¹, channel memory $I = 200$, and $N = 10^4$ users. After fixing (k, ϵ) and the MC parameters, we generate 100 random ground-truth distributions $\{\mathbf{p}^{(i)}\}_{i=1}^{100}$ by sampling uniformly from the probability simplex (implemented via a symmetric Dirichlet sampler). For each user U_j and each distribution index i , we draw $X_j^{(i)} \sim \mathbf{p}^{(i)}$ and apply the chosen ϵ -LDP mechanism to obtain a privatized report $Y_j^{(i)} \in \mathcal{Y}_m$ (where \mathcal{Y}_m denotes the output alphabet under method m), which is then mapped to a binary string via a method-specific encoding

$$\phi_m : \mathcal{Y}_m \rightarrow \{0, 1\}^{l_m}, \quad \mathbf{b}_{j,m}^{(i)} := \phi_m(Y_j^{(i)}), \quad (30)$$

where l_m is the (fixed) report length in bits under method m . For hashing-based mechanisms BLH and OLH, the report $Y_j^{(i)}$ and its resulting binary mapping contain both the randomized output and the corresponding randomly chosen hash vector, as detailed in Sections III-D and III-E.

For each user, we append the 100 binary reports into a single long binary sequence and transmit it contiguously. Formally, for user U_j and method m , we form the concatenation

$$\mathbf{b}_{j,m} := \text{concat}(\mathbf{b}_{j,m}^{(1)}, \mathbf{b}_{j,m}^{(2)}, \dots, \mathbf{b}_{j,m}^{(100)}) \in \{0, 1\}^{100 \cdot l_m}, \quad (31)$$

¹These simulation parameters are extensively used in the MC literature, representing a channel in which each transmitted and detected molecule is a human insulin hormone [15].

where $\text{concat}(\cdot)$ denotes vector concatenation. This is important because inter-symbol interference (ISI) is the major impairment in diffusion-based MC [15]: molecule arrivals from previous 1-bit transmissions affect the molecule counts in subsequent signal intervals. By transmitting long sequences, we fully capture ISI rather than resetting the channel between reports.

Different LDP mechanisms produce different report lengths and different numbers of 1-bits, both of which directly influence ISI. To ensure a fair comparison, we normalize the signal interval duration and the number of molecules emitted per 1-bit so that every method uses the same total transmission time and a comparable (i.e. close) total number of emitted molecules as the unprivatized baseline [16], [17]. Let W_m be the total number of 1-bits of all the users accumulated under method m :

$$W_m := \sum_{j=1}^N \sum_{t=1}^{100 \cdot l_m} \mathbf{1}\{b_{j,m}[t] = 1\} = \sum_{j=1}^N \sum_{t=1}^{100 \cdot l_m} b_{j,m}[t], \quad (32)$$

where $b_{j,m}[t] \in \{0, 1\}$ denotes the t -th transmitted bit in the concatenated sequence $\mathbf{b}_{j,m}$. With $m = 0$ denoting the unprivatized baseline, we set

$$t_{s,m} = t_{s,0} \cdot \frac{l_0}{l_m} \quad \text{and} \quad M_m = \lfloor M_0 \cdot \frac{W_0}{W_m} \rfloor. \quad (33)$$

This ensures $l_m t_{s,m} = l_0 t_{s,0}$ and $M_m W_m \approx M_0 W_0$ for all methods.

Given the transmitted bit sequence, we simulate the received molecule-count sequence using (5) with the multinomial channel model of Section II (via Gaussian counting noise with variance σ^2 , rounded to the nearest integer). We then apply threshold detection: a transmitted bit $b_{j,m}[t]$ is detected as $\hat{b}_{j,m}[t] = 1$ iff the observed molecule count in the corresponding interval is larger than or equal to a fixed threshold $\tau \in \mathbb{N}$. To ensure a reliable and consistent comparison across privacy schemes, we choose a single global threshold per method by minimizing the total BER aggregated across all users²:

$$\tau_m^* \in \arg \min_{\tau} \sum_{j=1}^N \text{Ham}(\hat{\mathbf{b}}_{j,m}(\tau), \mathbf{b}_{j,m}). \quad (34)$$

After detection, we split each user's detected bitstream back into 100 reports, invert the method-specific binary mapping³, and apply the corresponding unbiased estimator from Section III to obtain $\hat{\mathbf{p}}_m^{(i)}$ for each i . Finally, we compute the average ℓ_1 error:

$$\ell_1^m := \frac{1}{100} \sum_{i=1}^{100} \left\| \mathbf{p}^{(i)} - \hat{\mathbf{p}}_m^{(i)} \right\|_1. \quad (35)$$

²In practical MC receivers, the detection threshold is typically calibrated using a short training sequence. Here, to enable a maximally fair comparison, we instead use the globally optimal static threshold for each scheme.

³Because the MC channel can flip bits, the detected binary word may not correspond to any valid report (e.g., for OLH it may decode to $\hat{z} \notin \{0, \dots, g^{m+1} - 1\}$). In this case, we treat it as an invalid report and replace it by a uniformly random valid report before running the corresponding estimator.

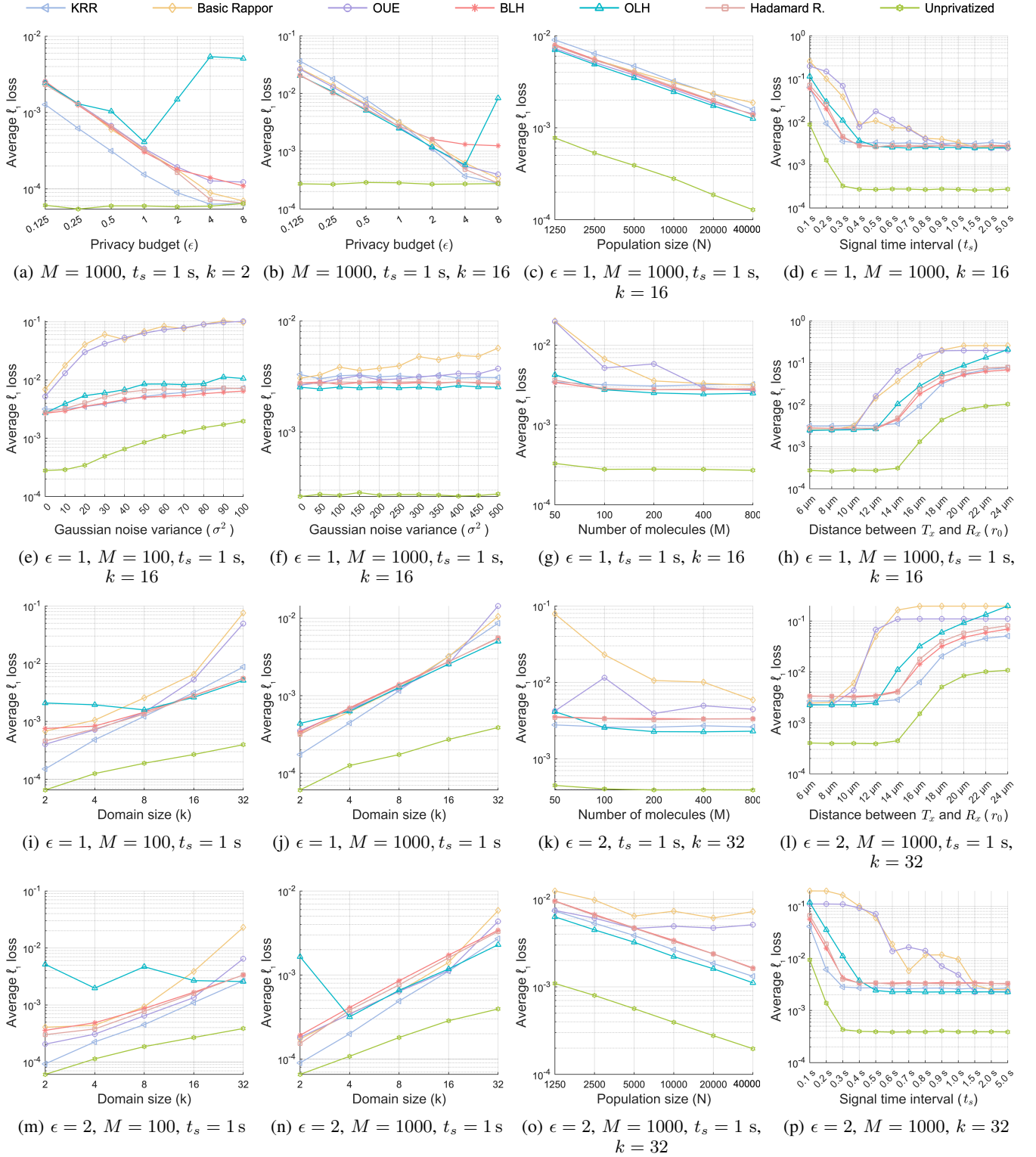


Fig. 3: Average ℓ_1 losses across methods. Unless stated otherwise, $D = 79.4 \mu\text{m}^2/\text{s}$, $r_R = 5 \mu\text{m}$, $r_0 = 10 \mu\text{m}$, $N = 10^4$, $\sigma^2 = 0$.

B. Evaluation of Simulation Results

Fig. 3 reports the average ℓ_1 error across the considered scenarios. Fig. 3(a,b,c) shows the performance across different privacy budgets (ϵ). We first observe that at larger ϵ values, OLH (which is equivalent to BLH for $\epsilon = 0.125$ and 0.25)

loses some of its advantage over other methods due to its diminishing signal interval duration. We focus on two representative privacy budgets, $\epsilon \in \{1, 2\}$, which are commonly used as benchmark values in empirical evaluations of LDP mechanisms [4].

For $\epsilon = 1$, as seen in Fig. 3(i,j), when t_s and M are sufficiently large, OLH becomes the most advantageous method for domain sizes $k \geq 16$, surpassing KRR (which otherwise outperforms the remaining methods). However, as shown in Fig. 3(d,g,h), when the channel quality deteriorates due to a smaller t_s , lower M , or a larger transmitter-receiver distance (Fig. 3(h)), KRR regains its advantage over OLH. This robustness occurs because KRR has a shorter report length ($l_{\text{KRR}} \leq l_{\text{OLH}}$), resulting in a larger normalized t_s and M values, which we omit for brevity, compared to OLH under the normalizations of Eq. (33).

For $\epsilon = 2$, a similar trend is observed. As shown in Fig. 3(m,n), given sufficiently large t_s and M , OLH outperforms KRR at domain sizes $k \geq 32$. Conversely, Fig. 3(k,l,p) demonstrates that as the transmission quality degrades (smaller t_s , lower M , or larger distance as in Fig. 3(l)), the larger normalized t_s and M of KRR allow it to once again surpass OLH.

Regarding the population size parameter N , Fig. 3(c,o) shows that the methods partially preserve their performance rankings relative to each other, with the estimation error reducing as N increases. We evaluate the impact of Gaussian counting noise variance (σ^2) in Fig. 3(e,f). The results indicate that the performance gap between the methods is mostly preserved under noise. As shown in Fig. 3(f), a larger molecule budget per 1-bit (e.g., $M = 1000$) significantly mitigates the adverse effects of counting noise. In contrast, for a lower budget of $M = 100$ (Fig. 3(e)), larger noise variance substantially degrades the communication quality across all mechanisms. As can be seen in Fig. 3 (h,l), when the distance between the transmitter and the receiver (r_0) surpasses 12 μm , the KRR method becomes more advantageous over the OLH method. In Fig. 3 (h), though BLH outperforms all other privacy schemes when the distance is larger than 18 μm , the overall reliability remains significantly poor.

Based on our simulated parameter grid, the performance trade-off between OLH and KRR depends heavily on channel quality. For instance, at distances of $r_0 \leq 12 \mu\text{m}$, OLH typically yields a lower estimation error when the unprivatized signal interval is approximately $t_s \geq 0.5 \text{ s}$ (given $M \geq 1000$) or $t_s \geq 1 \text{ s}$ (given $M \geq 100$). When the available channel resources fall below these empirical ranges, KRR generally provides a more robust alternative. A similar trend is observed for $\epsilon = 2$ and $k \geq 32$: OLH is again favored under comparable channel conditions, whereas KRR becomes advantageous as the channel conditions degrade.

V. RUN LENGTH LIMITED ISI MITIGATION LDP CODING (RLIM-LDP)

To enhance the reliability of the private MC channel, we propose *RLIM-LDP*, a unified framework integrating Local Differential Privacy (LDP) with the Run-Length-Limited ISI-Mitigation (RLIM) coding family introduced in [6]. While LDP mechanisms ensure privacy by randomizing user data, they do not inherently mitigate physical channel impairments such as inter-symbol interference (ISI) [15]. By encoding privatized reports via RLIM, we minimize the frequency of

molecular emissions, thereby optimizing the energy budget and reducing the final distribution estimation error ℓ_1 at the central server.

Let \mathcal{M} denote the chosen ϵ -LDP mechanism with output alphabet \mathcal{Y}_m . We observe that for every mechanism considered, the output can be represented as a vector of fixed length ℓ_m over a finite integer alphabet $\mathcal{A}_B = \{0, 1, \dots, B-1\}$. Specifically, $B = g$ for the Optimized Local Hashing (OLH) mechanism, and $B = 2$ for all other mechanisms considered (e.g., KRR, RAPPOR). We define the bijective indexing map $\phi_m : \mathcal{A}_B^{\ell_m} \rightarrow \{0, 1, \dots, B^{\ell_m} - 1\}$ as the positional interpretation of the output vector $\mathbf{y} = (y_1, y_2, \dots, y_{\ell_m}) \in \mathcal{Y}_m$:

$$\phi_m(\mathbf{y}) = \sum_{j=1}^{\ell_m} y_j \cdot B^{\ell_m - j}. \quad (36)$$

This mapping assigns a unique integer index s to each possible privatized report. Let $S_m = B^{\ell_m}$ denote the total cardinality of the report space.

To transmit these S_m privatized reports more reliably over the MC channel, we map them into a codebook $\mathcal{C}_m \subset \{0, 1\}^{n_m}$. Rather than using standard binary representations that are vulnerable to inter-symbol interference (ISI), we employ the enhanced version of Run-Length-Limited ISI-Mitigation (RLIM) coding as outlined in Section IV.B.5 in [6]. The core principle of RLIM is to enforce a minimum temporal spacing between molecular emissions while minimizing the overall frequency of those emissions. Let $\widehat{RLIM}_2(n_m)$ denote the space of all valid length- n_m binary sequences satisfying a $(2, \infty)$ -run-length constraint, meaning every 1-bit is strictly followed by at least two 0-bits. Here, the hat notation [6] explicitly indicates that the all-zero vector is permitted in the coding space.

For each LDP method m , we construct a corresponding channel codebook, defined as $\mathcal{C}_m \subset \widehat{RLIM}_2(n_m)$, by first determining the minimum codeword length n_m required to satisfy the cardinality condition $|\widehat{RLIM}_2(n_m)| \geq S_m$. From this feasible space, \mathcal{C}_m is formed by systematically selecting the S_m codewords with the lowest possible Hamming weight. As established in [6], this minimum-weight selection is advantageous: a sparser codebook minimizes the total number of 1-bits transmitted across the network. Under standard power normalizations, conserving this energy allows us to allocate a larger molecule budget to each individual 1-bit. This reduces bit error rate (BER), improving communication reliability [6]. The transmission process consists of mapping the privatized LDP report \mathbf{y} to its index $s = \phi_m(\mathbf{y})$ and transmitting the corresponding codeword $\mathbf{c}_s \in \mathcal{C}_m$.

A. RLIM-LDP Simulation Results

The data generation and physical channel configurations are identical to the LDP evaluation framework established in Section IV. Specifically, we generate 100 random k -ary ground-truth probability distributions. For each of the N users, we draw exactly one sample from each of the 100 distributions, resulting in a concatenated sequence of 100 consecutive transmissions per user. To ensure a fair comparison with the unprivatized baseline, we normalize the transmission

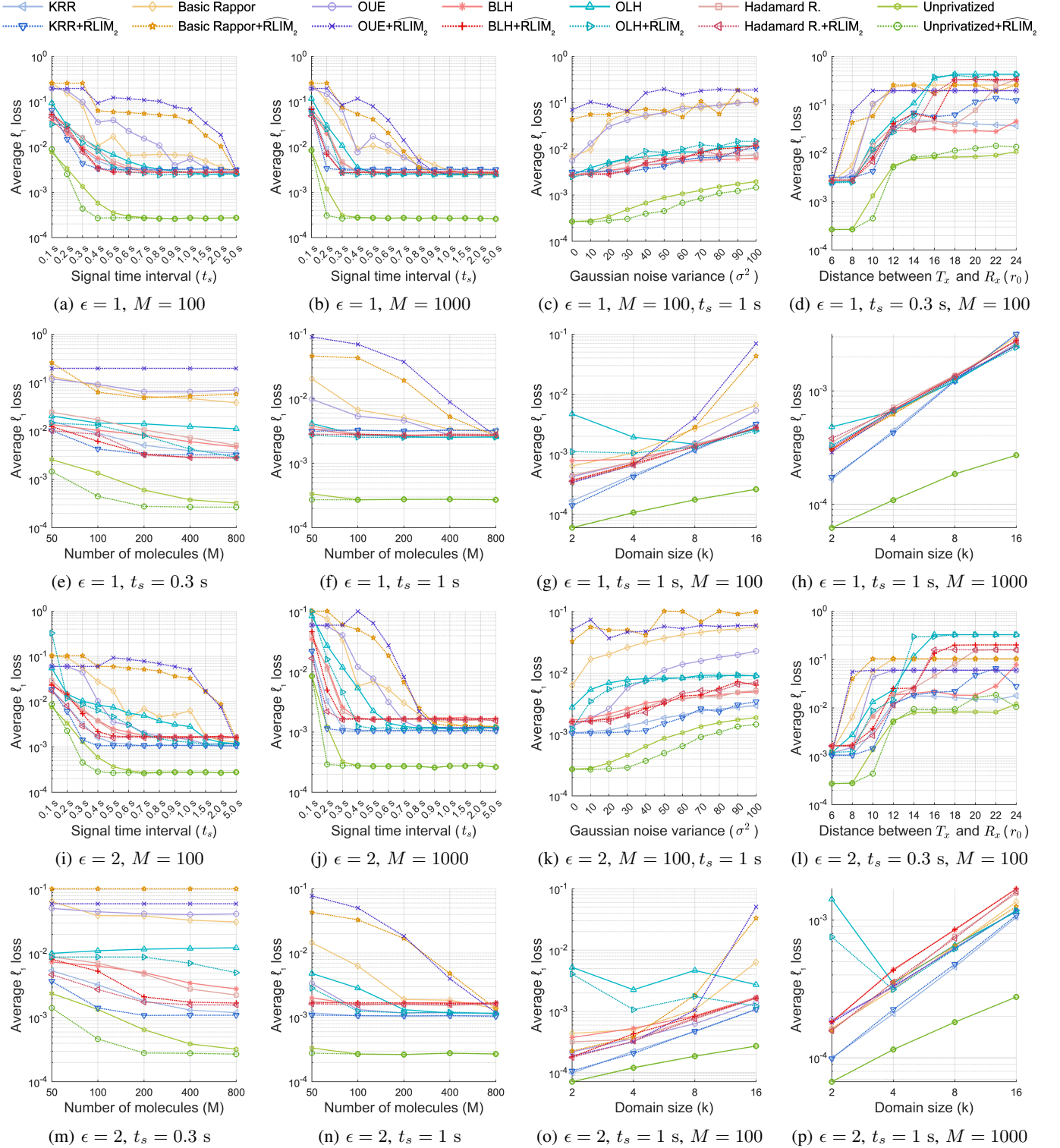


Fig. 4: Average ℓ_1 losses across methods. Unless stated otherwise, $k = 16$, $D = 79.4 \mu\text{m}^2/\text{s}$, $r_R = 5 \mu\text{m}$, $r_0 = 10 \mu\text{m}$, $N = 10^4$, $\sigma^2 = 0$.

parameters M and t_s across all methods. This guarantees a constant total transmission time and a strict preservation of the total emitted molecule budget across the network, as defined in Eq. (33).

At the receiver, absorbed molecules are counted and mapped to a binary sequence using a fixed threshold detector. Because

threshold optimization over the full population is computationally expensive due to the end-to-end decoding pipeline of RLIM codes, we instead perform a supervised calibration step using a pilot set \mathcal{K} comprising the first 100 users' transmissions. The detection threshold τ is optimized to minimize the end-to-end Symbol Error Rate (SER) over this calibration set

\mathcal{K} . For a given threshold τ , let $\hat{s}_k(\tau)$ denote the decoded index of the k -th transmission in the pilot set after applying RLIM error correction and decoding. The optimal threshold τ^* is given by:

$$\tau^* = \underset{\tau}{\operatorname{argmin}} \sum_{k \in \mathcal{K}} \mathbf{1} \{ \hat{s}_k(\tau) \neq s_k \}. \quad (37)$$

The detected sequence is then processed by the linear-time RLIM error correction algorithm, which enforces the $(2, \infty)$ -RLL constraint and is equivalent to a Viterbi decoder with the deterministic last-wins rule [6]. The corrected sequence is decoded to the estimated index \hat{s} , which is finally mapped back to the LDP report $\hat{y} = \phi_m^{-1}(\hat{s})$ and passed to the central server for aggregation.

For the privacy budgets $\epsilon \in \{1, 2\}$, the RLIM-LDP simulation results are presented in Fig. 4. We first observe in Fig. 4(a, b, i, j) that, with the exception of Basic RAPPOR and OUE (which consistently yield the highest estimation error throughout this study), RLIM coding noticeably improves the average ℓ_1 loss when the signal interval duration is small. In particular, the gain is most pronounced for $t_s \in \{0.1, 0.2, 0.3, 0.4, 0.5\}$ s (and remains visible at $t_s = 0.6$ s in several cases). As t_s increases, the performance of both the RLIM-coded and uncoded methods gradually converges.

Regarding the impact of Gaussian counting noise variance (σ^2), the RLIM-coded schemes maintain a clear advantage over their uncoded counterparts under moderate noise conditions (e.g., up to $\sigma^2 = 30$ in Fig. 4(c), and $\sigma^2 = 50$ in Fig. 4(k)), again excluding Basic RAPPOR and OUE. Furthermore, Fig. 4(d,l) shows that RLIM coding improves reliability for distances up to $r_0 = 10 \mu\text{m}$, while Basic RAPPOR and OUE are again the main exceptions. At $r_0 = 12 \mu\text{m}$, gains remain visible for OLH.

Overall, the integration of RLIM channel coding provides a substantial performance advantage to the most competitive LDP mechanisms, effectively reducing the lowest achievable ℓ_1 distribution-estimation error under limited channel resources. Within our simulated parameters, this improvement is particularly significant for shorter signal intervals ($t_s \leq 0.5$ s), moderate communication distances ($r_0 \leq 10 \mu\text{m}$), and under moderate receiver counting-noise variance.

VI. CONCLUSION

This paper investigated the integration of local differential privacy (LDP) into diffusion-based molecular communication (MC) networks. By benchmarking state-of-the-art LDP mechanisms under realistic channel conditions, we demonstrated that mechanisms with higher statistical accuracy often generate longer binary reports, which exacerbate inter-symbol interference and degrade communication reliability. Consequently, our findings indicate that while Optimized Local Hashing (OLH) minimizes distribution-estimation error when channel resources are ample and the alphabet size is moderate to large, the shorter report lengths of the k -ary Randomized Response (KRR) mechanism provide superior robustness when transmission conditions degrade.

To maintain these privacy guarantees under severe nanoscale physical constraints, we proposed the RLIM-LDP architecture.

Extensive simulations demonstrated that encoding privatized LDP reports with run-length-limited ISI-mitigation (RLIM) coding effectively yields significant improvements in end-to-end reliability and estimation accuracy under tight time and molecule resource constraints. Overall, this work demonstrates that private, population-scale aggregate data analysis can be reliably achieved in diffusive biological environments under practical in-body MC channel conditions.

REFERENCES

- [1] M. Kescu, E. Dinc, B. A. Bilgin, H. Ramezani, and O. B. Akan, "Transmitter and receiver architectures for molecular communications: A survey on physical design with modulation, coding, and detection techniques," *Proceedings of the IEEE*, vol. 107, no. 7, pp. 1302–1341, 2019.
- [2] V. Loscrí, C. Marchal, N. Mitton, G. Fortino, and A. V. Vasilakos, "Security and privacy in molecular communication and networking: Opportunities and challenges," *IEEE Transactions on NanoBioscience*, vol. 13, no. 3, pp. 198–207, 2014.
- [3] V. Gholamiyan, Y. Zhao, W. Labidi, H. Boche, and C. Deppe, "Security and privacy: Key requirements for molecular communication in medicine and healthcare," 2025. [Online]. Available: <https://arxiv.org/abs/2503.11169>
- [4] T. Wang, J. Blocki, N. Li, and S. Jha, "Locally differentially private protocols for frequency estimation," in *26th USENIX Security Symposium (USENIX Security 17)*. Vancouver, BC: USENIX Association, Aug. 2017, pp. 729–745. [Online]. Available: <https://www.usenix.org/conference/usenixsecurity17/technical-sessions/presentation/wang-tianhao>
- [5] G. Cormode, S. Maddock, and C. Maple, "Frequency estimation under local differential privacy," *Proc. VLDB Endow.*, vol. 14, no. 11, p. 2046–2058, Jul. 2021. [Online]. Available: <https://doi.org/10.14778/3476249.3476261>
- [6] M. Şahin and O. B. Akan, "Run-length-limited isi-mitigation (rlim) coding for molecular communication," *IEEE Transactions on Molecular, Biological, and Multi-Scale Communications*, pp. 1–1, 2026.
- [7] M. S. Kuran, H. B. Yilmaz, T. Tugcu, and I. F. Akyildiz, "Modulation techniques for communication via diffusion in nanonetworks," in *2011 IEEE International Conference on Communications (ICC)*, 2011, pp. 1–5.
- [8] O. B. Akan, H. Ramezani, T. Khan, N. A. Abbasi, and M. Kescu, "Fundamentals of molecular information and communication science," *Proceedings of the IEEE*, vol. 105, no. 2, pp. 306–318, 2017.
- [9] H. B. Yilmaz, A. C. Heren, T. Tugcu, and C.-B. Chae, "Three-dimensional channel characteristics for molecular communications with an absorbing receiver," *IEEE Communications Letters*, vol. 18, no. 6, pp. 929–932, 2014.
- [10] F. Vakiliipoor, L. Barletta, S. Bregni, and M. Magarini, "Correlated source achievable information rate analysis in diffusive channels with memory," in *2024 IEEE Latin-American Conference on Communications (LATINCOM)*, 2024, pp. 1–6.
- [11] K. Aliqab, I. Nadeem, and S. R. Khan, "A comprehensive review of in-body biomedical antennas: Design, challenges and applications," *Micromachines*, vol. 14, no. 7, 2023. [Online]. Available: <https://www.mdpi.com/2072-666X/14/7/1472>
- [12] P. Kairouz, K. Bonawitz, and D. Ramage, "Discrete distribution estimation under local privacy," in *Proceedings of The 33rd International Conference on Machine Learning*, ser. Proceedings of Machine Learning Research, M. F. Balcan and K. Q. Weinberger, Eds., vol. 48. New York, New York, USA: PMLR, 20–22 Jun 2016, pp. 2436–2444. [Online]. Available: <https://proceedings.mlr.press/v48/kairouz16.html>
- [13] U. Erlingsson, V. Pihur, and A. Korolova, "Rappor: Randomized aggregatable privacy-preserving ordinal response," in *Proceedings of the 2014 ACM SIGSAC Conference on Computer and Communications Security*, ser. CCS '14. New York, NY, USA: Association for Computing Machinery, 2014, p. 1054–1067. [Online]. Available: <https://doi.org/10.1145/2660267.2660348>
- [14] J. Acharya, Z. Sun, and H. Zhang, "Hadamard response: Estimating distributions privately, efficiently, and with little communication," in *Proceedings of the Twenty-Second International Conference on Artificial Intelligence and Statistics*, ser. Proceedings of Machine Learning Research, K. Chaudhuri and M. Sugiyama, Eds., vol. 89. PMLR, 16–18 Apr 2019, pp. 1120–1129. [Online]. Available: <https://proceedings.mlr.press/v89/acharya19a.html>

- [15] B. Tepekule, A. E. Pusane, H. B. Yilmaz, C.-B. Chae, and T. Tugcu, "Isi mitigation techniques in molecular communication," *IEEE Transactions on Molecular, Biological and Multi-Scale Communications*, vol. 1, no. 2, pp. 202–216, 2015.
- [16] M. Şahin, B. E. Ortlek, and O. B. Akan, "Molecular arithmetic coding (moac) and optimized molecular prefix coding (mopc) for diffusion-based molecular communication," *IEEE Transactions on Molecular, Biological, and Multi-Scale Communications*, vol. 11, no. 1, pp. 66–77, 2025.
- [17] M. C. Gursoy, E. Basar, A. E. Pusane, and T. Tugcu, "Index modulation for molecular communication via diffusion systems," *IEEE Transactions on Communications*, vol. 67, no. 5, pp. 3337–3350, 2019.



Melih Şahin (Graduate Student Member, IEEE) is a PhD student in the Department of Engineering at the University of Cambridge. He received an MS in Electrical and Electronics Engineering with thesis in 2025 and a BSc in Computer Engineering with a Mathematics minor and an AI track in 2024 at Koç University, after his first year of undergraduate studies at KAIST. His notable distinctions include an Intel ISEF 4th place Grand Award in Mathematics in 2018. His research interests cover Information Theory, Coding Theory, and Molecular Communication.



Ozgur B. Akan (Fellow, IEEE) received the PhD from the School of Electrical and Computer Engineering Georgia Institute of Technology Atlanta, in 2004. He is currently the Head of Internet of Everything (IoE) Group, with the Department of Engineering, University of Cambridge, UK and the Director of Centre for neXt-generation Communications (CXC), Koç University, Türkiye. His research interests include wireless, nano, and molecular communications and Internet of Everything.